Interactions of solitons with positive and negative masses: Shuttle motion and coacceleration

Hidetsugu Sakaguchi[1] and Boris A. Malomed[2]

[1]*Department of Applied Science for Electronics and Materials, Interdisciplinary Graduate School of Engineering Sciences,*
Kyushu University, Kasuga, Fukuoka 816-8580, Japan
[2]*Department of Physical Electronics, School of Electrical Engineering, Faculty of Engineering, and Center for Light-Matter Interaction,*
Tel Aviv University, Tel Aviv 69978, Israel

We consider a possibility to realize self-accelerating motion of interacting states with effective positive and negative masses in the form of pairs of solitons in two-component BEC loaded in an optical-lattice (OL) potential. A crucial role is played by the fact that gap solitons may feature a negative dynamical mass, keeping their mobility in the OL. First, the respective system of coupled Gross-Pitaevskii equations (GPE) is reduced to a system of equations for envelopes of the lattice wave functions. Two generic dynamical regimes are revealed by simulations of the reduced system, viz., shuttle oscillations of pairs of solitons with positive and negative masses, and splitting of the pair. The coaccelerating motion of the interacting solitons, which keeps constant separation between them, occurs at the boundary between the shuttle motion and splitting. The position of the coacceleration regime in the system's parameter space can be adjusted with the help of an additional gravity potential, which induces its own acceleration, that may offset the relative acceleration of the two solitons, while gravity masses of both solitons remain positive. The numerical findings are accurately reproduced by a variational approximation. Collisions between shuttling or coaccelerating soliton pairs do not alter the character of the dynamical regime. Finally, regimes of the shuttle motion, coacceleration, and splitting are corroborated by simulations of the original GPE system, with the explicitly present OL potential.

I. INTRODUCTION

Search for robust self-accelerating pulses in various physical settings has drawn much interest, starting from the discovery of Airy-wave modes in quantum mechanics [1]. Experimentally, this propagation mode was demonstrated in quantum matter represented by electron beams (under conditions which make interactions between electrons negligible) [2]. Using the similarity of the linear Schrödinger equation for the wave function of quantum particles to the paraxial wave-propagation equation in classical-field systems, the realization of Airy waves was elaborated in optics [3], plasmonics [4], gas discharge [5], acoustics [6], and hydrodynamics [7]. Further, the commonly known similarity of the Schrödinger equation to the Gross-Pitaevskii equation (GPE) for the mean-field wave function of atomic Bose-Einstein condensates (BECs) makes it possible to predict Airy-wave modes in atomic BEC as well [8].

Full Airy waves carry an infinite norm (alias diverging integral power, in terms of optics); therefore truncated waves with a finite norm were used in the theory and experiments [3,9], although the truncation leads to gradual destruction of the self-accelerating wave pattern. The medium's nonlinearity may also be detrimental to the evolution of the Airy waves, which are introduced as eigenmodes of the linear propagation [9–11].

For these reasons, a relevant objective is to design physical models that would allow self-accelerated propagation of well-localized modes with a finite norm, which would be maintained by the nonlinearity rather than being damaged

by it. Actually, this objective implies looking for models that should support stable self-acceleration of quasisoliton states. In particular, this possibility was recently predicted for one- and two-dimensional hybrid (matter wave–microwave) solitons produced by the interplay of a two-component BEC and a resonant electromagnetic field which couples the components [12]. Another approach relies on the well-known idea that a pair of objects with positive and negative masses may develop constant self-acceleration under the action of interaction forces [13]. While real bodies with a negative mass do not exist, quasiparticles and wave pulses may acquire an effective negative mass in various settings. In this direction, as essential result was the prediction [14] and experimental realization [15] of bound pulses in nonlinear photonic crystals with opposite signs of the dispersion (effective mass) of their two components. Theoretically, a similar result was predicted for a pair of correlated quantum particles coupled by long-range interaction, which perform hopping in a Bose-Hubbard lattice, as one of the particles may also acquire an effective negative mass in the lattice [16].

The objective of the present work is to explore a possibility of forming bound states of solitons with opposite signs of the effective masses, which implies that they should also have opposite signs of the self-interaction coefficients (otherwise, bright solitons cannot exist in both components; for this reason, only one component was a soliton in the above-mentioned photonic setting [14], while the other one was treated as a Thomas-Fermi mode). This situation is possible in a two-component atomic BEC loaded in an optical-lattice (OL) potential, which may induce the effective mass of

either sign (positive for regular solitons, and negative for gap solitons in a finite bandgap [17–25]), while the sign of the self-interaction in any component may be switched by means of the Feshbach resonance [26]. It is relevant to mention that the dynamics of a pair of matter-wave solitons with effective masses of opposite signs, loaded in a harmonic-oscillator trapping potential, was studied in recent work [25]. As a result, the soliton with the positive mass remains trapped, while its counterpart with the negative mass can escape, as the potential is effectively expulsive for it [20].

The model is introduced in Sec. II, first in the form of the nonlinearly coupled GPEs with spatially periodic potentials representing the OL [23]. Then, we apply the approximation of slowly varying envelope amplitudes to derive a free-space GPE system with opposite effective masses and opposite signs of the self-interaction. In Sec. III, simulations of the latter system demonstrate that it gives rise to two generic dynamical regimes: spontaneous shuttle oscillations of pairs of interacting solitons, with the separation between them also oscillating (so that the solitons periodically pass through each other), and splitting of the pair. The coacceleration of the positive- and negative-mass solitons, which keep a constant distance between themselves, takes place at the boundary between the two regimes (a similar observation suggesting the non-generic character of the coaccelerating motion of the pair of interacting pulses, one of which was not a soliton, was reported in Ref. [14]; however, the generic regime of the shuttle motion was not reported in that work). Note that the shuttle regime also implies that the two soliton stay paired and spontaneously develop common acceleration, but with a periodically reversing sign. Also in Sec. III, we develop a variational approximation (VA), which accurately predicts the shuttle, coacceleration, and splitting regimes. Further, in the same section we consider the system which additionally includes a gravity potential (it is important to note that, while the effective dynamical mass of one soliton is negative, its gravity mass remains normal positive). Using the fact that the gravity also imparts acceleration to the solitons, we demonstrate, both numerically and by means of the VA, that the gravity-induced acceleration can offset the splitting force, and thus adjust the location of the coacceleration regime in the system's parameter space. In addition, we report results of simulation of collisions between soliton pairs, in both the shuttle and coacceleration regimes, the result being that the collisions may change the separation between the paired solitons, but not the character of the dynamical regime. Finally, in Sec. IV we return to the underlying system of GPEs which explicitly includes the OL potential, and demonstrate, by means of systematic simulations, that the same regimes, viz., the shuttle motion, coacceleration, and splitting, are produced by that system, including its extended version with the gravity potential. The paper is concluded by Sec. V.

II. MODELS: THE OPTICAL LATTICE AND SLOWLY VARYING ENVELOPES

We start with the system of scaled GPEs for a binary BEC, with equal atomic masses of its two components, ϕ and ψ, loaded in the OL potential, whose period is scaled to be 1,

with amplitudes $-U_{1,2}$ [23]:

$$i\frac{\partial \phi}{\partial t} = -\frac{1}{2}\frac{\partial^2 \phi}{\partial x^2} - [g_1|\phi|^2 + \gamma|\psi|^2 + U_1\cos(2\pi x)]\phi,$$

$$i\frac{\partial \psi}{\partial t} = -\frac{1}{2}\frac{\partial^2 \psi}{\partial x^2} - [\gamma|\phi|^2 - g_2|\psi|^2 + U_2\cos(2\pi x)]\psi. \quad (1)$$

Here $g_1 > 0$ and $-g_2 < 0$ are coefficients of the self-interaction of the components, implying that, as stated above, their signs are made opposite by means of the Feshbach resonance applied to one of the components, and $\gamma > 0$ is the coefficient of the cross-attraction. It is well known that the GPEs, based on the mean-field approximation, provide a very accurate model of the atomic BEC. The only exception occurs in the case of a binary atomic BEC, when the self-repulsion in both components almost exactly cancels with attraction between them, making the beyond-mean-field terms, generated by quantum fluctuations, important corrections to the GPE system [18]. This is definitely not the case in the present setting.

To focus on the case of opposite signs of the effective mass for solitons in the interacting components, ϕ and ψ, we consider the case when quasi–wave numbers of wave functions ϕ and ψ are set to be close, respectively, to the center and edge of the first OL's Brillouin zone, in terms of Eq. (1). Near the center, which corresponds to the zero quasi–wave number, the effective mass, calculated by means of the known methods [19,20,23], is

$$M_1 = \frac{2\pi^3 + U_1^2 + \pi^2\sqrt{4\pi^4 + 2U_1^2}}{10\pi^4 + U_1^2 - 3\pi^2\sqrt{4\pi^4 + 2U_1^2}}, \quad (2)$$

and the wave function itself is approximated as

$$\phi(x) = \Phi(x)\frac{1 + 2a\cos(2\pi x)}{\sqrt{1 + 2a^2}}, \quad (3)$$

$$a \equiv \sqrt{\left(\frac{\pi^2}{U_1}\right)^2 + \frac{1}{2}} - \frac{\pi^2}{U_1}, \quad (4)$$

where $\Phi(x)$ is the slowly varying envelope amplitude. Near the edge of the Brillouin zone, which corresponds to quasi-wave number π, the effective mass is

$$-M_2 = \frac{U_2}{U_2 - 2\pi^2} \quad (5)$$

(it is defined with sign minus, to focus below on the relevant case of the negative mass, $M_2 > 0$), with the respective wave function

$$\psi(x) = \sqrt{2}\Psi(x)\cos(\pi x) \quad (6)$$

and slowly varying envelope amplitude $\Psi(x)$. The slow variation implies that solitons represented by Φ and Ψ may be relevant solutions if their width l is much larger than periods of spatial oscillations of the carrier wave functions (3) and (6), i.e.,

$$l \gg 1. \quad (7)$$

The substitution of expressions (3) and (6) into original equations (1) leads, by means of the procedure of averaging

with respect to rapid oscillations of the carrier wave functions [20,23], to equations governing the slow evolution of the envelope amplitudes, which do not include an external potential:

$$i\frac{\partial \Phi}{\partial t} = -\frac{1}{2M_1}\frac{\partial^2 \Phi}{\partial x^2} - (G_1|\Phi|^2 + \Gamma|\Psi|^2)\Phi, \qquad (8)$$

$$i\frac{\partial \Psi}{\partial t} = \frac{1}{2M_2}\frac{\partial^2 \Psi}{\partial x^2} - (\Gamma|\Phi|^2 - G_2|\Psi|^2)\Psi, \qquad (9)$$

with effective nonlinearity coefficients,

$$G_1 = g_1\frac{1 + 12a^2 + 6a^4}{(1 + 2a^2)^2}, \quad G_2 = \frac{3}{2}g_2,$$

$$\Gamma = \frac{1 + 2a^2 + 2a}{1 + 2a^2}. \qquad (10)$$

Numerical results are reported below both for the reduced system of Eqs. (8) and (9) (in Sec. III) and for the underlying one, based on Eq. (1) (in Sec. IV).

The minus sign is eliminated in front of the second derivative in Eq. (9) according to the definition of the respective effective mass in Eq. (5). Accordingly, it is obvious that Eqs. (8) and (9) may indeed feature opposite signs of the effective masses, if M_1 and M_2 are both positive (or both negative), and opposite signs of the effective coefficients of the self-interaction in the two components, if G_1 and G_2 are both positive (or both negative), too. These sign combinations open the way to the creation of pairs of bright solitons with opposite signs of their dynamical masses, which is the objective outlined in the Introduction. We also fix $\Gamma > 0$, although the sign of this coefficient can be reversed by a combination of the complex conjugation and swap $\Phi \rightleftarrows \Psi$. Note that Eqs. (8) and (9) keep the Galilean invariance, in spite of opposite signs of the mass parameters in them; therefore, it is easy to find soliton complexes moving with an arbitrary velocity, as shown below.

III. DYNAMICS OF PAIRED ENVELOPE SOLITONS: NUMERICAL AND ANALYTICAL RESULTS

A. Exact solutions for soliton complexes

In the basic case of $M_{1,2} > 0$ and $G_{1,2} > 0$, Eqs. (8) and (9) generate, in addition to obvious single-component solitons, a family of exact steady-state soliton complexes with free parameter κ (the inverse width) and an arbitrary velocity, v:

$$\Phi = \frac{A\exp\left[iM_1vx - \frac{i}{2}\left(\frac{\kappa^2}{M_1} + M_1v^2\right)t\right]}{\cosh[\kappa(x - vt)]}, \qquad (11)$$

$$\Psi = \frac{B\exp\left[-iM_2vx + \frac{i}{2}\left(\frac{\kappa^2}{M_2} + M_2v^2\right)t\right]}{\cosh[\kappa(x - vt)]}, \qquad (12)$$

$$A^2 = \frac{\kappa^2}{M_1M_2}\frac{M_2G_2 - M_1\Gamma}{G_1G_2 + \Gamma^2}, \qquad (13)$$

$$B^2 = \frac{\kappa^2}{M_1M_2}\frac{M_1G_1 + M_2\Gamma}{G_1G_2 + \Gamma^2}, \qquad (14)$$

provided that expressions (13) and (14) take positive values. It is relevant to mention that this solution represents

only a particular case of a more general family of stationary two-component solitons, as, in the case of $v = 0$, the generic soliton solution must feature two independent parameters, which may be defined as norms of the two components,

$$N_{1,2} = \int_{-\infty}^{+\infty} |\Phi(x), \Psi(x)|^2 dx, \qquad (15)$$

while the exact solution (11) and (12) contains only one free parameter, κ, at $v = 0$. If Eqs. (8) and (9) are derived from the underlying GPEs by means of the above-mentioned averaging procedure, then the corresponding condition (7) amounts to restriction $\kappa \ll 1$. However, the scaling invariance of Eqs. (8) and (9) implies that simulations of the equations may be actually performed for $\kappa = 1$ (as it is done below), and the results can be then rescaled for any other value of κ.

In accordance with what is reported below for soliton pairs with a finite separation between their constituents, the steady-state complexes are stable under condition $\beta > 0$ imposed on the two components, see Eq. (18) below. In the opposite case of $\beta < 0$, the complexes are unstable against splitting into separating components.

B. Initial numerical results: Shuttle and self-accelerating motion of paired solitons

The soliton complexes given by Eqs. (11)–(14) do not feature self-acceleration, as they are built of two components which are located at the bottom of the potential of their mutual attraction, hence no interaction forces act on them. As stated above, our main objective is to look for self-accelerating soliton pairs. This may be possible if the constituents are separated by some distance, which gives rise to opposite interaction forces applied to them. Acting on the solitons with opposite signs of the dynamical mass, these forces should produce accelerations with identical signs.

To realize this possibility, we started simulations of Eqs. (8) and (9) for the soliton complexes given by Eqs. (11) and (12) with $\kappa = 1$ and $v = 0$, choosing other parameters as

$$M_1 = 1, \quad G_1 = 0.9, \quad \Gamma = 0.1, \quad G_2 = 0.1 + M_2^{-1}, \quad (16)$$

while M_2^{-1} will be varied as a control parameter. In this case, Eqs. (13) and (14) yield $A = B = 1$. The separation between the constituents, x_0, which is necessary to introduce the interaction forces, was introduced by taking the initial conditions as

$$\Phi_0 = \operatorname{sech} x, \quad \Psi_0 = \operatorname{sech}(x - x_0), \quad x_0 = 0.1, \quad (17)$$

whose norms (15) are $N_1 = N_2 = 2$. The simulations were performed with periodic boundary conditions, taking the period which is much larger than widths of the produced solitons, as seen in Fig. 1(a).

Figure 1 shows the evolution of the wave functions, in terms of $|\Phi(x, t)|$ and $|\Psi(x, t)|$ at (a) $M_2^{-1} = 1$ and (b) $M_2^{-1} = 0.96$. Permanent self-acceleration of the bound soliton pair is observed in Fig. 1(a). However, this regime of motion is not a generic one, in terms of varying control parameter M_2^{-1} (a conclusion that such a regime is not generic
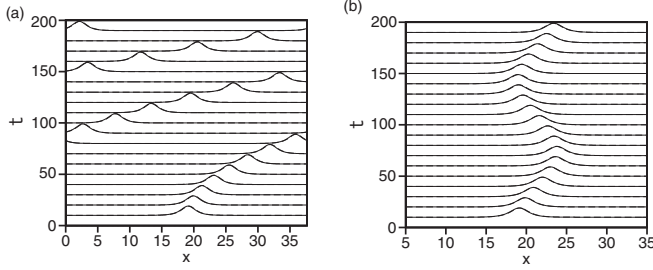
FIG. 1. The evolution of $|\Phi(x, t)|$ and $|\Psi(x, t)|$ (solid and dashed lines, respectively, which nearly overlap) at $M_2^{-1} = 1$ (a) and $M_2^{-1} = 0.96$ (b), with other parameters and the input taken as per Eqs. (16) and (17), respectively.

was also made in Ref. [14]): As shown in Fig. 1(b), the interacting solitons exhibit shuttle motion, with periodically sign-changing coacceleration, at $M_2^{-1} < 1$. The shuttle period diverges at $M_2^{-1} \to 1$, and the solitons separate at $M_2^{-1} > 1$. These conclusions are confirmed by Fig. 2(a), which displays trajectories of the motion of centers of both constituent solitons at $M_2^{-1} \leqslant 1$. Collecting results of simulations carried out at other values of the parameters suggests that, in the general case, the permanent coacceleration occurs under a balance condition,

$$\beta \equiv \frac{N_2}{M_1} - \frac{N_1}{M_2} = 0, \qquad (18)$$

which is derived below analytically by means of the VA.

Fixing the parameters as per Eq. (16) and $M_2^{-1} = 0.96$, the initial separation x_0 between the constituent solitons in Eq. (17) is varied in Fig. 2(b). It is observed that the shuttle motion persists in this case, with the amplitude growing proportionally to x_0 (the same result is derived below by means of the VA). On the other hand, the two solitons separate in the case of $M_2^{-1} > 1$.

Thus, the coacceleration regime plays the role of a separatrix between two generic regimes of motion, viz., the shuttle oscillations and splitting of the soliton pair. These conclusions, suggested by the systematic simulations, are explained by means of the VA developed below.
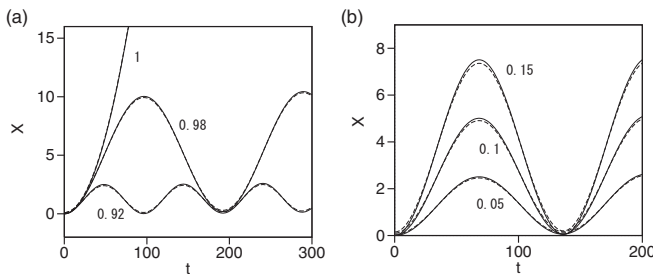

FIG. 2. Trajectories of centers of the Φ and Ψ components (solid and dashed lines, respectively): (a) at $M_2^{-1} = 0.92, 0.98$, and 1 for $x_0 = 0.1$ in Eq. (17) and (b) at $x_0 = 0.05, 0.10$, and 0.15 for fixed $M_2^{-1} = 0.96$.

C. The variational approximation and comparison with numerical results

The system of Eqs. (8) and (9) for envelope wave functions can be derived from the Lagrangian,

$$L = \int_{-\infty}^{+\infty} dx \left[\frac{i}{2} \left(\frac{\partial \Phi}{\partial t} \Phi^* - \frac{\partial \Phi^*}{\partial t} \Phi + \frac{\partial \Psi}{\partial t} \Psi^* - \frac{\partial \Psi^*}{\partial t} \Psi \right) \right.$$
$$- \frac{1}{2M_1} \left| \frac{\partial \Phi}{\partial x} \right|^2 + \frac{1}{2M_2} \left| \frac{\partial \Psi}{\partial x} \right|^2$$
$$\left. + \left(\frac{G_1}{2} |\Phi|^4 - \frac{G_2}{2} |\Psi|^4 + \Gamma |\Phi|^2 |\Psi|^2 \right) \right]. \qquad (19)$$

The solitons with amplitudes $A_{1,2}$, coordinates $\xi_{1,2}$, momenta $k_{1,2}$, and overall phases $\varphi_{1,2}$ may be approximated by the usual Gaussian ansatz [27,28]:

$$\{\Phi, \Psi\} = A_{1,2} \exp\{i\varphi_{1,2}(t) - \alpha_{1,2}[x - \xi_{1,2}(t)]^2$$
$$+ ik_{1,2}(t)(x - \xi_{1,2})\}. \qquad (20)$$

The substitution of the ansatz in Eq. (19) leads to the effective Lagrangian,

$$L_{\text{eff}} = -N_1 \dot{\varphi}_1 - N_2 \dot{\varphi}_2 + \frac{N_1}{2M_1} \alpha_1 + \frac{N_2}{2M_2} \alpha_2$$
$$+ \frac{G_1}{2} \sqrt{\frac{\alpha_1}{\pi}} N_1^2 - \frac{G_2}{2} \sqrt{\frac{\alpha_2}{\pi}} N_2^2$$
$$+ \Gamma \sqrt{\frac{2\alpha_1 \alpha_2}{\pi(\alpha_1 + \alpha_2)}} N_1 N_2 \exp\left[-\frac{2\alpha_1 \alpha_2}{\alpha_1 + \alpha_2} (\xi_1 - \xi_2)^2 \right]$$
$$- \frac{N_1}{2M_1} k_1^2 + \frac{N_2}{2M_2} k_2^2 + N_1 k_1 \dot{\xi}_1 + N_2 k_2 \dot{\xi}_2, \qquad (21)$$

where the overdot stands for d/dt and amplitudes $A_{1,2}$ are expressed in terms of the respective norms, $N_1 = \sqrt{\pi/(2\alpha_1)}A_1^2$ and $N_2 = \sqrt{\pi/(2\alpha_2)}A_2^2$. Being dynamical invariants of the system, the norms are treated as constants. The Lagrangian gives rise to the system of the Euler-Lagrange equations, which, on the elimination of $\dot{k}_{1,2}$, can be cast in the form of two coupled second-order equations of motion for coordinates $\xi_{1,2}$ (unessential equations for $\dot{\varphi}_{1,2}$ are not written here):

$$\frac{d^2 \xi_{1,2}}{dt^2} = \frac{N_{2,1}}{M_{1,2}} \alpha \exp\left[-\frac{2\alpha_1 \alpha_2}{\alpha_1 + \alpha_2} (\xi_1 - \xi_2)^2 \right] (\xi_2 - \xi_1), \qquad (22)$$

with

$$\alpha \equiv \frac{2\Gamma}{\sqrt{\pi}} \left(\frac{2\alpha_1 \alpha_2}{\alpha_1 + \alpha_2} \right)^{3/2}. \qquad (23)$$

It is seen that the right-hand sides of Eq. (22) for ξ_1 and ξ_2 have identical signs in the case of $M_1 M_2 > 0$ (recall we are dealing with the case of $M_{1,2} > 0$), which indeed implies the coacceleration of the solitons. That is, the first soliton, denoted by ξ_1, is attracted to the second soliton denoted by ξ_2, while the latter one is repelled from the first soliton. On the other hand, the total momentum of the soliton pair is as follows from Lagrangian (21):

$$P = N_1 M_1 \frac{d\xi_1}{dt} - N_2 M_2 \frac{d\xi_2}{dt}, \qquad (24)$$

and it immediately follows from Eq. (22) that P remains a dynamical invariant, even if the pair as a whole is moving with acceleration.

It is straightforward to combine Eqs. (22) for ξ_1 and ξ_2, deriving an equation for separation $\Delta\xi = \xi_2 - \xi_1$ between the solitons:

$$\frac{d^2\Delta\xi}{dt^2} = -\alpha\beta \exp\left[-\frac{2\alpha_1\alpha_2}{\alpha_1 + \alpha_2}(\Delta\xi)^2\right]\Delta\xi, \qquad (25)$$

where β is defined as per Eq. (18). In particular, for small $|\Delta\xi|$ the linearization of Eq. (25) yields

$$\frac{d^2\Delta\xi}{dt^2} = -\alpha\beta\Delta\xi. \qquad (26)$$

It follows from Eq. (26) that, in the case of $\alpha\beta > 0$ [i.e., $\Gamma\beta > 0$, as it follows from Eq. (23)], the separation between the interacting solitons preforms periodic oscillations with arbitrary amplitude x_0,

$$\Delta\xi = x_0 \cos(\sqrt{\alpha\beta}t), \qquad (27)$$

while in the opposite case, $\alpha\beta < 0$, the separation monotonously grows in time, i.e., the interacting solitons separate. The latter analytical result provides a direct explanation to the separation regime revealed above by the numerical simulations of Eqs. (8) and (9) at $\beta < 0$.

Exactly at $\beta = 0$, separation $\Delta\xi$ keeps the initial value, x_0, hence Eq. (22) predicts permanent coacceleration of the paired solitons, with the acceleration itself proportional to the initial separation, x_0. This analytical result explains the most essential numerical finding reported above: the coaccelerating motion of the internally stationary soliton pair at $\beta = 0$.

To address the shuttle motion revealed by the simulations in Figs. 1 and 2 at $\beta > 0$, we note that the linearized version of Eq. (22) gives rise to the following equation of motion for the mean position of the pair, $\Xi \equiv (\xi_1 + \xi_2)/2$:

$$\frac{d^2\Xi}{dt^2} = \frac{\alpha}{2}\left(\frac{N_2}{M_1} + \frac{N_1}{M_2}\right)\Delta\xi$$
$$= \frac{\alpha}{2}\left(\frac{N_2}{M_1} + \frac{N_1}{M_2}\right)x_0 \cos(\sqrt{\beta\alpha}t), \qquad (28)$$

where solutions (27) for $\Delta\xi$ is substituted. Then, the solution to Eq. (28) is

$$\Xi = Rx_0[1 - \cos(\sqrt{\beta\alpha}t)], \qquad (29)$$

$$R \equiv (2\beta)^{-1}\left(\frac{N_2}{M_1} + \frac{N_1}{M_2}\right), \qquad (30)$$

if the initial value of Ξ and overall velocity are zero. This result explains the shuttle motion of the soliton pair observed in Figs. 1 and 2, as well as the above-mentioned fact, also revealed by the direct simulations, that the amplitude of the shuttle oscillations grows proportionally to x_0. Further, in the limit of $\beta \to 0$, Eq. (28) precisely reproduces the permanent coacceleration of the pair, which was revealed by the direct simulations close to $\beta = 0$:

$$\Xi(\beta = 0) = \frac{1}{2}a_0t^2, \quad a_0 \equiv \frac{1}{2}\left(\frac{N_2}{M_1} + \frac{N_1}{M_2}\right)\alpha x_0. \qquad (31)$$
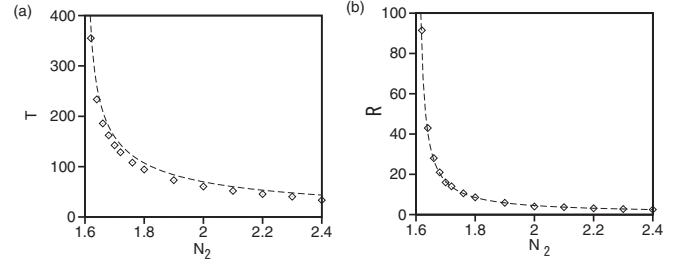

FIG. 3. (a) Rhombuses represent the numerically obtained period of oscillations of separation $\Delta\xi$ between the interacting solitons, as a function of norm N_2 for $N_1 = 2$, and other parameters taken as per Eq. (33). The dashed line shows the analytical prediction provided by Eq. (27), i.e., $T = 2\pi/\sqrt{\alpha\beta}$. (b) Rhombuses: The numerically evaluated ratio R of the oscillation amplitudes of the mean position of the soliton pair, Ξ, and separation $\Delta\xi$ between them. The dashed line shows the respective analytical approximation given by Eq. (30).

If full Eq. (22) is used, without the linearization, the acceleration is

$$a_0 = \frac{1}{2}\left(\frac{N_2}{M_1} + \frac{N_1}{M_2}\right)\alpha \exp\left(-\frac{2\alpha_1\alpha_2}{\alpha_1 + \alpha_2}x_0^2\right)x_0. \qquad (32)$$

The predictions of the VA are compared to numerical findings in Fig. 3, where Fig. 3(a) shows the numerically obtained period of oscillations of the separation between centers of the interacting solitons, in the case of $\beta > 0$, as a function of norm N_2. The numerical data are obtained using initial condition $\Phi_0(x) = \mathrm{sech}\,x$, $\Psi = \sqrt{N_2/2}\mathrm{sech}[\sqrt{N_2/2}(x - x_0)]$, with $x_0 = 0.1$, other parameters being

$$M_1 = 1, \quad M_2^{-1} = 0.8, \quad G_1 = G_2 = 0.9, \quad \Gamma = 0.1. \qquad (33)$$

The comparison of the analytically predicted period of the oscillations of separation $\Delta\xi$ between the solitons, see Eq. (27), and ratio R of the amplitude of the shuttle oscillations of the pair as a whole to the amplitude of the intrinsic oscillations of $\Delta\xi(t)$, see Eq. (30), with their numerically found counterparts attests to good accuracy of the analytical approximation. In particular, large values of R explain why the two solitons seem overlapping in Figs. 1(b) and 2.

Systematic results for the coaccelerating motion of the pair of solitons at $\beta = 0$ are displayed in Fig. 4. Figure 4(a) shows a typical example of numerically generated trajectories of their centers for parameters

$$M_1 = M_2^{-1} = 1, \quad G_1 = 0.9, \quad G_2 = 1.1,$$
$$\Gamma = 0.1, \quad N_1 = N_2 = 2, \qquad (34)$$

and initial separation $x_0 = 0.5$. Further, the dependence of the numerically identified acceleration on initial separation x_0 and its comparison with the analytical prediction produced by Eq. (32) are displayed in Fig. 4(b). The presence of the maximum in the dependence $a_0(x_0)$ (at point $x_0 = 1.05$) is explained by the fact that the interaction force vanishes both at $x_0 = 0$ and at $x_0 \to \infty$.
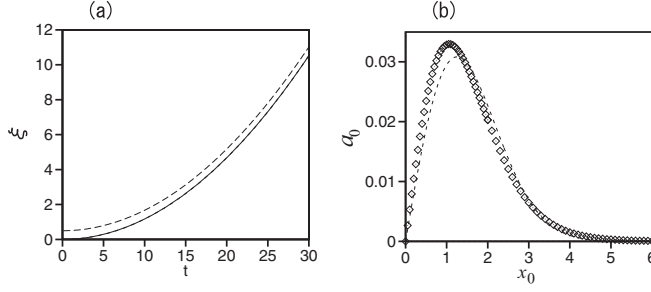
FIG. 4. (a) The continuous and dashed curves display a typical example of numerically generated trajectories of centers of the interacting solitons, in the case of their coaccelerating motion. The respective parameters are given in Eq. (34), with $x_0 = 0.5$. Both trajectories are close to parabolas, with acceleration $a_0 = 0.0234$. (b) Rhombuses represent numerically found values of the coacceleration, a_0, as a function of x_0, for the same parameters, the dashed curve showing the analytical approximation given by Eq. (32).

D. The coaccelerating motion of the envelope soliton pair in the presence of gravity

Because the gravity also imparts acceleration to matter-wave solitons [29], a natural extension of the above analysis is to add the gravity potential, $-fx$, with strength f, to the system of Eqs. (8) and (9):

$$i\frac{\partial \Phi}{\partial t} = -\frac{1}{2M_1}\frac{\partial^2 \Phi}{\partial x^2} - (G_1|\Phi|^2 + \Gamma|\Psi|^2 + fx)\Phi, \quad (35)$$

$$i\frac{\partial \Psi}{\partial t} = -\frac{1}{2M_2}\frac{\partial^2 \Psi}{\partial x^2} - (-G_2|\Psi|^2 + \Gamma|\Phi|^2 + fx)\Psi. \quad (36)$$

We stress that, while the derivation of Eqs. (8) and (9) and then (35) and (36) from the underlying GPE system (1), including the OL potential (and the gravity potential, in the present context), may generate the negative effective dynamical mass, $-M_2$, gravity masses of the solitons represented by envelope wave functions Φ and Ψ remains normal (positive); therefore, the gravity potentials have the same sign in Eqs. (35) and (36).

The VA outlined above can be readily extended to include the gravity, which yields the following modification of Eq. (22):

$$\frac{d^2\xi_1}{dt^2} = \frac{N_2}{M_1}\alpha \exp\left[-\frac{2\alpha_1\alpha_2}{\alpha_1+\alpha_2}(\xi_1-\xi_2)^2\right](\xi_2-\xi_1) + \frac{f}{M_1}, \quad (37)$$

$$\frac{d^2\xi_2}{dt^2} = \frac{N_1}{M_2}\alpha \exp\left[-\frac{2\alpha_1\alpha_2}{\alpha_1+\alpha_2}(\xi_1-\xi_2)^2\right](\xi_2-\xi_1) - \frac{f}{M_2}, \quad (38)$$

and respective changes in Eqs. (25) and (28):

$$\frac{d^2\Delta\xi}{dt^2} = -\alpha\beta \exp\left[-\frac{2\alpha_1\alpha_2}{\alpha_1+\alpha_2}(\Delta\xi)^2\right]\Delta\xi$$

$$- \left(\frac{1}{M_2}+\frac{1}{M_1}\right)f, \quad (39)$$

$$\frac{d^2\Xi}{dt^2} = \frac{\alpha}{2}\left(\frac{N_2}{M_1}+\frac{N_1}{M_2}\right)\exp\left[-\frac{2\alpha_1\alpha_2}{\alpha_1+\alpha_2}(\Delta\xi)^2\right]\Delta\xi$$

$$+ \frac{1}{2}\left(\frac{1}{M_1}-\frac{1}{M_2}\right)f. \quad (40)$$

The gravity may be used to compensate the splitting force in the case of $\beta < 0$ and thus switch the splitting regime into the coacceleration. A straightforward analysis demonstrates that the balance between the interaction and gravity forces produces a stable coacceleration regime at $\Delta\xi > 1.05$, where the slope of the curve in Fig. 4(b) is negative. As a typical example, Figs. 5(a) and 5(b) show trajectories of centers of the coaccelerating solitons, and the evolution of the separation between them at $f = 0$ and $f = 6.1 \times 10^{-5}$, for parameters

$$M_1 = 1, \quad M_2^{-1} = 1.01, \quad G_1 = 0.9, \quad G_2 = 1.11,$$
$$\Gamma = 0.1, \quad N_1 = N_2 = 2, \quad (41)$$

and initial separation $x_0 = 2.5$. It is seen that the gravity maintains the stable coacceleration. On the other hand, in the absence of the gravity, the solitons exhibit, in Fig. 5(b), slow separation.

Further, Fig. 5(c) shows the gravity strength in the stable coaccelerating pair as a function of the initial separation, x_0, as found from numerical data, and compared to the analytical prediction, which is produced by Eq. (39):

$$f = -\frac{M_1M_2\alpha}{M_1+M_2}\exp\left(-\frac{2\alpha_1\alpha_2}{\alpha_1+\alpha_2}x_0^2\right)x_0\beta. \quad (42)$$

Note that the inverse relation, $\beta = -(M_1M_2\alpha x_0)^{-1}(M_1+M_2)\exp[2\alpha_1\alpha_2(\alpha_1+\alpha_2)^{-1}x_0^2]f$, defines the value of β at which the robust regime of the coacceleration occurs, replacing condition $\beta = 0$ [see Eq. (18)], derived above in the absence of gravity. Thus, the gravity may be used to adjust the occurrence of the coacceleration regime for given values of other parameters (in particular, β). The necessary value of f can be readily tuned by varying the angle, θ, between the vertical axis and direction of the quasi-one-dimensional waveguide into which the BEC is loaded: $f = f_{max}\cos\theta$, where f_{max} corresponds to the waveguide oriented parallel to the gravity force.

E. Collisions between pairs of envelope solitons

Another relevant issue is to consider collisions between the soliton complexes. Typical examples, produced by simulations of Eqs. (8) and (9) (in the absence of the gravity), are displayed in Fig. 6, starting from the corresponding input,

$$\Phi_0(x) = \text{sech}(x - L/4) + \text{sech}(x - 3L/4),$$
$$\Psi_0(x) = \text{sech}(x - L/4 - x_0) + \text{sech}(x - 3L/4 + x_0),$$
$$x_0 = 0.1, \quad L = 12\pi \quad (43)$$

(this input implies that the integration-domain's center is located at point $x = L/2$).

First, for parameters

$$M_1 = 1, \quad M_2^{-1} = 0.98, \quad G_1 = 0.9,$$
$$G_2 = 1.06, \quad \Gamma = 0.1, \quad (44)$$

at which the pair of interacting solitons perform the shuttle motion, Fig. 6(a) demonstrates that the two pairs collide

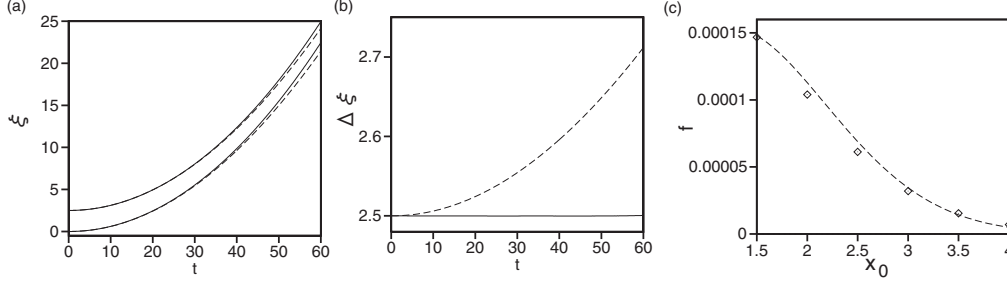FIG. 5. (a) Numerically obtained trajectories of centers ξ_1 and ξ_2 of the interacting solitons in the absence and presence of the gravity, viz., at $f = 0$ and $f = 6.1 \times 10^{-5}$ (the dashed and continuous lines, respectively) for parameter given by Eq. (41). (b) The evolution of the separation between the solitons, $\Delta\xi$, in the same cases. (c) Rhombuses represent numerically found values of the gravity strength, f, corresponding to stable pairs of coaccelerating solitons, as a function of the initial separation between them, x_0. The dashed curve is the respective analytical prediction, produced by Eq. (42).

and bounce back. Detailed analysis of the numerical data demonstrates that the collision result in an increase of the separation $\Delta\xi$ in each pair and, respectively, increase of the amplitude of the shuttle oscillations.

The collision between two soliton pairs which move with the coacceleration in opposite directions is displayed in Fig. 6(b) for parameters

$$M_1 = 1, \quad M_2^{-1} = 1, \quad G_1 = 0.9, \quad \Gamma = 0.1, \quad G_2 = 1.1. \tag{45}$$

In this case the colliding pairs pass through each other and, similarly to the case displayed in Fig. 6(a), the collision results in an increase of the separation between the interacting solitons in each pair, from $\Delta\xi = 0.10$ to $\Delta\xi \approx 0.17$. This, in turn, leads to the increase of the coacceleration, as per Eq. (32) and Fig. 4(b). The enhanced self-acceleration is clearly observed in Fig. 6(b).

IV. COACCELERATING SOLITON PAIRS IN THE UNDERLYING SYSTEM WITH THE OPTICAL-LATTICE POTENTIAL

The above considerations, both numerical and analytical, were performed for Eqs. (8) and (9), which govern the evolution of envelope wave functions $\Phi(x, t)$ and $\Psi(x, t)$. It is also relevant to verify the possibility of the shuttle and coaccelerating motion of the soliton pairs in the framework of the underlying GPEs (1), which explicitly include the OL

FIG. 6. Collisions of solitons pairs, generated by initial conditions (43). (a) Pairs performing shuttle motion at parameters given by Eq. (44). (b) Coaccelerating pairs, corresponding to parameters (45). In both panels, profiles of $|\Phi(x, t)|$ and $|\Psi(x, t)|$ strongly overlap.

potential and original physical coefficients, rather than the effective ones produced by averaging, as given by Eqs. (2), (5), and (10). We also consider the version of Eq. (1) which includes the gravity potential, similarly to Eqs. (35) and (36):

$$i\frac{\partial\phi}{\partial t} = -\frac{1}{2}\frac{\partial^2\phi}{\partial x^2} - [g_1|\phi|^2 + \gamma|\psi|^2 + U_1\cos(2\pi x) + fx]\phi,$$

$$i\frac{\partial\psi}{\partial t} = -\frac{1}{2}\frac{\partial^2\psi}{\partial x^2} - [\gamma|\phi|^2 - g_2|\psi|^2 + U_2\cos(2\pi x) + fx]\psi. \tag{46}$$

Note that gravity strength f in Eq. (46) is the same as in Eqs. (8) and (9), because the derivation of the latter equations from the former ones does not involve rescaling of variables t and x.

Equations (1) and (46) were solved numerically with various initial conditions. In particular, input

$$\phi_0(x) = A\frac{1 + 2a\cos(\pi x)}{\sqrt{1 + 2a^2}}\mathrm{sech}[A(x - 0.5)],$$

$$\psi_0(x) = \sqrt{2}B\cos(\pi x)\mathrm{sech}(Bx), \tag{47}$$

with a defined as per Eq. (4), is suggested by the above approximations (3) and (6) for the wave functions.

First, Fig. 7 displays numerical results obtained by simulations of Eq. (1) with initial conditions (47) in the case of $U_1 = 0$ and $U_2 = 8$, that is, assuming that the OL potential acts only on the ψ component (typical results for the setting with $U_1 = U_2$ are displayed below). Figure 7(a) shows trajectories of the motion of centers of the two components for parameters

$$g_1 = 0.8, \quad \gamma = 0.2, \quad g_2 = \frac{2}{3}\left(\gamma + \frac{2\pi^2 - U_2}{U_2}\right) \equiv 1.11 \tag{48}$$

in Eq. (1), and amplitude $B = 0.15$ in Eq. (47), while amplitude A is varied, taking values $A = 0.075, 0.094$, and 0.15 [the particular choice of g_2 in Eq. (48) is made to facilitate the prediction of the value of A at which the coaccelerating regime may be expected, see Eq. (50)]. The choice of the smallest amplitude, $A = 0.075$, gives rise to the shuttle motion, while the largest amplitude, $A = 0.15$, leads to splitting of the soliton pair. The regime of the robust coacceleration of the two solitons, which keep a constant separation
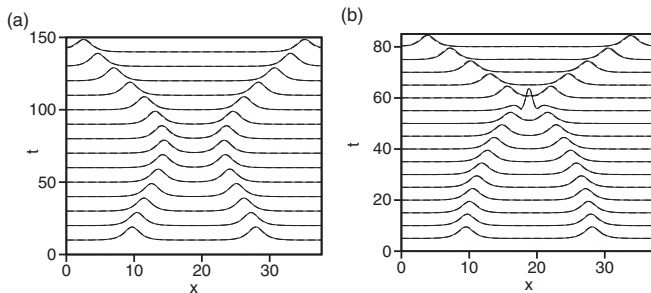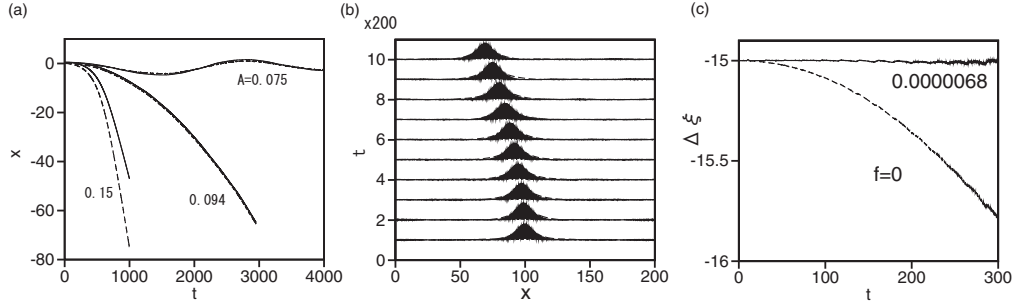
FIG. 7. (a) The continuous and dashed lines represent trajectories of the motion of centers of components ϕ and ψ, produced by simulations of Eq. (1) with $U_1 = 0$, $U_2 = 8$ and input (47), in which $B = 0.15$ is fixed, while values $A = 0.075$, 0.094, and 0.150 are adopted for the other amplitude. (b) The evolution of (virtually coinciding) $|\phi(x,t)|$ and $|\psi(x,t)|$ for $A = 0.094$. (c) The evolution of separation $\Delta\xi$ between the interacting components at $A = 0.110$ and $x_0 = 15$ in the absence of the gravity (the dashed line) and in the presence of the gravity potential with strength $f = -6.8 \times 10^{-6}$ (the solid line), as produced by simulations of Eqs. (46), which include both the OL and gravity potentials. Other parameters are fixed according to Eq. (48).

between themselves, is found at

$$A = A_0^{(num)} \approx 0.094. \qquad (49)$$

The analytical approximation, based on the above condition $\beta = 0$ [see Eq. (18)], with effective mass and interaction coefficients calculated as per Eqs. (2), (5), and (10), yields the value

$$A_0 = BU_2/(2\pi^2 - U_2) = 0.102, \qquad (50)$$

at which the coaccelerating regime is predicted, the respective negative effective mass being $-M_2 = -A_0/B = -0.6266$. A difference ($\Delta A_0/A_0 \approx 0.08$) of the predicted value (50) from its numerical counterpart (49) is explained by deviation of the analytical approximations (2) and (5) from numerically exact values, and also by effects of the emission of radiation from the solitons moving through the periodic potential.

Figure 7(b) shows the evolution of wave functions in the coaccelerating pair, in terms of $|\phi(x,t)|$ and $|\psi(x,t)|$, at point (49). The pair of solitons are traveling to the left, under the action of the attraction between them, because the positive-mass ϕ soliton is initially set to the right of the negative-mass one in the ψ component. If the initial configuration is reversed, then the pair moves to right. At $A > 0.094$, the pair splits because the negative-mass soliton runs to left with a larger acceleration than the positive-mass one is able to develop. On the other hand, at $A < 0.094$ the positive-mass soliton overtakes the negative-mass one and passes it, which leads to reversal of the direction of motion, inducing the shuttle regime.

The effect of the gravity potential, added to Eq. (46), is displayed in Fig. 7(c). It shows the evolution of separation $\Delta\xi$ between solitons' centers for $A = 0.11$ in input (47), with initial separation $x_0 = 15$. According to the above findings, in the absence of the gravity the pair should split in this case, because amplitude A exceeds the respective critical value, $A_0 = 0.094$. This is indeed demonstrated by the dashed curve in Fig. 7(c). On the other hand, the solid curve shows that the application of gravity with $f = -6.8 \times 10^{-6}$ offsets the splitting force and creates a coaccelerating pair with a virtually constant separation, cf. Fig. 5(b).

A typical example of the robust coacceleration regime found in the system with equal amplitudes of the OL

potential acting on both components, viz., $U_1 = U_2 = 13$, is displayed in Fig. 8. In this case, the amplitudes of input (47) are $A = 0.103$ and $B = 0.15$, and the self-interaction coefficients are taken as $g_1 = (1 + 2a^2)^2/(1 + 12a^2 + 6a^4)[1/M_1 - \gamma(1 + 2a^2)/(1 + 2a^2 + 2a)] \equiv 0.348$ and $g_2 = (2/3)[1/M_2 + \gamma(1 + 2a^2)/(1 + 2a^2 + 2a)] \equiv 0.368$, for $\gamma = 0.05$, where a is defined by Eq. (4). In the framework of the above analytical approximation, these parameters predict the coaccelerating motion at $\beta = 0$ [see Eq. (18)], which amounts to the value of the amplitude $A_0 = BM_2/M_1 = 0.158$. It is essentially larger than the numerically found value, $A_0^{(num)} \approx 0.103$, at which the coacceleration is observed in Fig. 8, i.e., in this case, with the strong OL potential, the simple analytical approximation produces only qualitatively correct predictions.

Last, while the dynamical regimes of the shuttle motion and coacceleration produced by Eqs. (8) and (9), or (35) and (36), may persist indefinitely, the motion of the solitons across the OL in the framework of Eqs. (1) and (46) is accompanied by weak radiation losses, which may be seen as tiny perturbations in Figs. 7 and 8. Eventually, these losses may essentially damage the solitons, but this will happen on a timescale essentially exceeding an experimentally relevant one.
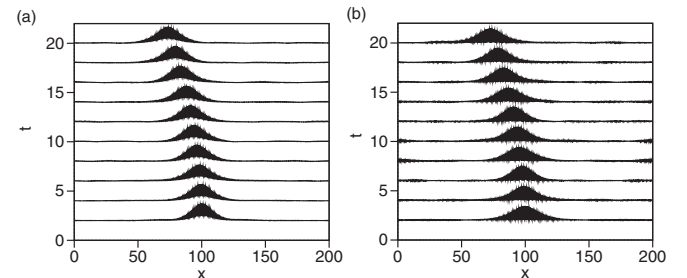

FIG. 8. The evolution of $|\phi(x,t)|$ (a) and $|\psi(x,t)|$ (b), produced by simulations of Eq. (1) with $g_1 = 0.348$, $g_2 = 0.368$, $\gamma = 0.05$, and $U_1 = U_2 = 13$, and initial conditions (47) with $A = 0.103$ and $B = 0.15$. The robust regime of the coacceleration of the interacting positive- (ϕ) and negative- (ψ) mass solitons is observed.

V. CONCLUSION

The objective of this work is to establish the framework which admits coaccelerating motion of interacting objects with opposite signs of the effective mass, using pairs of matter-wave solitons which move against the background of the OL potential. The effective negative mass of one component is provided by the known property of gap solitons. Reducing the full system of the GPEs, which includes the OL potential, to equations for slowly varying envelopes, systematic simulations and the VA (variational approximation) reveal two generic dynamical regimes, viz., spontaneous shuttle oscillations of the mean position of the soliton pair, in the course of which the solitons periodically pass through each other, and splitting of the pair. The robust coacceleration of the soliton pairs, with a permanent separation between the constituents, is found at the boundary between these two regimes. The location of the boundary can be adjusted by dint of the gravity potential added to the system. The VA accurately predicts all these effects. Finally, the same dynamical regimes, including the robust coacceleration, are directly demonstrated by simulations of the underlying system, which includes the OL potential and the gravity potential (if any) as well. The predicted effects can be realized experimentally in two-component atomic BEC, loaded in a quasi-one-dimensional waveguide combined with the OL, and the occurrence of the coacceleration regime can be adjusted by choosing the angle between the waveguide and gravity direction.

It may be interesting to consider a modification of the model which includes linear interconversion (Rabi coupling) between the components, which may help to additionally bind them, cf. Ref. [30]. A challenging possibility is to develop a two-dimensional version of the present system and, accordingly, to study pairs of two-dimensional solitons in the regimes of coacceleration and spontaneous shuttle motion.

Finally, it is also relevant to mention that, in addition to the ultracold atomic gases, exciton-polariton BECs have been experimentally realized in semiconductor microcavities [31,32], and predicted in graphene and similar two-dimensional materials [33,34], at temperatures exceeding those necessary for the condensation of bosonic gases by eight or nine orders of magnitude. Polariton solitons have also been created in microcavities [35], and it is expected that they may exist in graphene-like settings as well [36]. These findings suggest a possibility to create coupled positive- and negative-mass soliton pairs in polariton BEC. However, the necessary analysis will be completely different from that reported in the present paper, as media supporting polaritons are essentially dissipative, and hence a pump must be included, too. The latter term (unlike the simple dissipation) destroys the Galilean invariance, thus making the consideration of accelerating and shuttle dynamical regimes a challenging problem, which should be considered elsewhere.

[1] M. V. Berry and N. L. Balazs, Am. J. Phys. **47**, 264 (1979).

[2] N. Voloch-Bloch, Y. Lereah, Y. Lilach, A. Gover, and A. Arie, Nature **494**, 331 (2013).

[3] G. A. Siviloglou and D. N. Christodoulides, Opt. Lett. **32**, 979 (2007); G. A. Siviloglou, J. Broky, A. Dogariu, and D. N. Christodoulides, Phys. Rev. Lett. **99**, 213901 (2007); Opt. Lett. **33**, 207 (2008); R. El-Ganainy, K. G. Makris, M. A. Miri, D. N. Christodoulides, and Z. Chen, Phys. Rev. A **84**, 023842 (2011); P. Rose, F. Diebel, M. Boguslawski, and C. Denz, Appl. Phys. Lett. **102**, 101101 (2013); R. Driben, Y. Hu, Z. Chen, B. A. Malomed, and R. Morandotti, Opt. Lett. **38**, 2499 (2013); N. K. Efremidis, Phys. Rev. A **89**, 023841 (2014).

[4] A. Salandrino and D. N. Christodoulides, Opt. Lett. **35**, 2082 (2010); A. Minovich, A. E. Klein, N. Janunts, T. Pertsch, D. N. Neshev, and Y. S. Kivshar, Phys. Rev. Lett. **107**, 116802 (2011); L. Li, T. Li, S. M. Wang, C. Zhang, and S. N. Zhu, *ibid.* **107**, 126804 (2011); I. Epstein and A. Arie, *ibid.* **112**, 023903 (2014); A. Libster-Hershko, I. Epstein, and A. Arie, *ibid.* **113**, 123902 (2014); A. E. Minovich, A. E. Klein, D. N. Neshev, T. Pertsch, Y. S. Kivshar, and D. N. Christodoulides, Laser Phot. Rev. **8**, 221 (2014).

[5] M. Clerici, Y. Hu, P. Lassonde, C. Milian, A. Couairon, D. N. Christodoulides, Z. Chen, L. Razzari, F. Vidal, F. Legare, D. Faccio, and R. Morandotti, Sci. Adv. **1**, 1400111 (2015).

[6] P. Zhang, T. Li, J. Zhu, X. Zhu, S. Yang, Y. Wang, X. Yin, and X. Zhang, Nat. Commun. **5**, 4316 (2014); U. Bar-Ziv, A. Postan, and M. Segev, Phys. Rev. B **92**, 100301(R) (2015).

[7] S. Fu, Y. Tsur, J. Zhou, L. Shemer, and A. Arie, Phys. Rev. Lett. **115**, 034501 (2015).

[8] N. K. Efremidis, V. Paltoglou, and W. von Klitzing, Phys. Rev. A **87**, 043637 (2013); C. Yuce, Mod. Phys. Lett. B **29**, 1550171 (2015).

[9] P. Panagiotopoulos, D. Abdollahpour, A. Lotti, A. Couairon, D. Faccio, D. G. Papazoglou, and S. Tzortzakis, Phys. Rev. A **86**, 013842 (2012).

[10] T. Ellenbogen, N. Voloch-Bloch, A. Ganany-Padowicz, and A. Arie, Nat. Photonics **3**, 395 (2009); S. Jia, J. Lee, J. W. Fleischer, G. A. Siviloglou, and D. N. Christodoulides, Phys. Rev. Lett. **104**, 253904 (2010); D. Abdollahpour, S. Suntsov, D. G. Papazoglou, and S. Tzortzakis, *ibid.* **105**, 253901 (2010); Y. Hu, S. Huang, P. Zhang, C. Lou, J. Xu, and Z. Chen, Opt. Lett. **35**, 3952 (2010); I. Kaminer, M. Segev, and D. N. Christodoulides, Phys. Rev. Lett. **106**, 213903 (2011); A. Lotti, D. Faccio, A. Couairon, D. G. Papazoglou, P. Panagiotopoulos, D. Abdollahpour, and S. Tzortzakis, Phys. Rev. A **84**, 021807 (2011); Y. Fattal, A. Rudnick, and D. M. Marom, Opt. Express **19**, 17298 (2011); A. Rudnick and D. M. Marom, *ibid.* **19**, 25570 (2011); P. Zhang, Y. Hu, D. Cannan, A. Salandrino, T. Li, R. Morandotti, X. Zhang, and Z. Chen, Opt. Lett. **37**, 2820 (2012); I. Kaminer, J. Nemirovsky, and M. Segev, Opt. Express **20**, 18827 (2012); I. Dolev, I. Kaminer, A. Shapira, M. Segev, and A. Arie, Phys. Rev. Lett. **108**, 113903 (2012); R. Driben, V. V. Konotop, and T. Meier, Opt. Lett. **39**, 5523 (2014); I. M. Allayarov and E. N. Tsoy, Phys. Rev. A **90**, 023852 (2014).

[11] T. Mayteevarunyoo and B. A. Malomed, Opt. Lett. **40**, 4947 (2015); **41**, 2919 (2016); J. Opt. **19**, 085501 (2017).

[12] J. Qin, Z. Liang, B. A. Malomed, and G. Dong, arXiv:1901.02325.

[13] R. L. Forward, J. Propul. Power **6**, 28 (1990); M. G. Millis, *ibid.* **13**, 577 (1997).

[14] S. Batz and U. Peschel, Phys. Rev. Lett. **110**, 193901 (2013).

[15] M. Wimmer, A. Regensburger, C. Bersch, M.-A. Miri, S. Batz, G. Onishchukov, D. N. Christodoulides, and U. Peschel, Nat. Phys. **9**, 780 (2013).

[16] S. Longhi, New J. Phys. **16**, 113076 (2014).

[17] V. V. Konotop and M. Salerno, Phys. Rev. A **65**, 021602 (2002); G. L. Alfimov, V. V. Konotop, and M. Salerno, Europhys. Lett. **58**, 7 (2002); B. B. Baizakov, V. V. Konotop, and M. Salerno, J. Phys. B **35**, 5105 (2002).

[18] D. S. Petrov, Phys. Rev. Lett. **115**, 155302 (2015); D. S. Petrov and G. E. Astrakharchik, *ibid.* **117**, 100401 (2016).

[19] H. Pu, L. O. Baksmaty, W. Zhang, N. P. Bigelow, and P. Meystre, Phys. Rev. A **67**, 043605 (2003).

[20] H. Sakaguchi and B. A. Malomed, J. Phys. B **37**, 1443 (2004).

[21] E. A. Ostrovskaya and Y. S. Kivshar, Opt. Express **12**, 19 (2004).

[22] B. Eiermann, Th. Anker, M. Albiez, M. Taglieber, P. Treutlein, K.-P. Marzlin, and M. K. Oberthaler, Phys. Rev. Lett. **92**, 230401 (2004).

[23] V. A. Brazhnyi and V. V. Konotop, Mod. Phys. Lett. B **18**, 627 (2004); O. Morsch and M. Oberthaler, Rev. Mod. Phys. **78**, 179 (2006).

[24] Yu. V. Bludov, V. V. Konotop, and M. Salerno, Opt. Lett. **36**, 2856 (2011).

[25] Yu. V. Bludov and M. A. García-Ñustes, J. Phys. B **50**, 135004 (2017).

[26] C. Chin, R. Grimm, P. Julienne, and E. Tiesinga, Rev. Mod. Phys. **82**, 1225 (2010).

[27] D. Anderson, Phys. Rev. A **27**, 3135 (1983).

[28] B. A. Malomed, Prog. Opt. **43**, 71 (2002).

[29] O. Zobay and B. M. Garraway, Phys. Rev. A **69**, 023605 (2004); Q. Yang and J. F. Zhang, Opt. Commun. **258**, 35 (2006); M. Fattori, C. D'Errico, G. Roati, M. Zaccanti, M. Jona-Lasinio, M. Modugno, M. Inguscio, and G. Modugno, Phys. Rev. Lett. **100**, 080405 (2008); A. Mohamadou, E. Wamba, S. Y. Doka, T. B. Ekogo, and T. C. Kofane, Phys. Rev. A **84**, 023602 (2011); N. V. Vysotina and N. N. Rosanov, G. A. Sekh, Phys. Lett. A **381**, 852 (2017); B. A. Malomed, N. N. Rosanov, and S. V. Fedorov, Phys. Rev. E **97**, 052204 (2018).

[30] M. I. Merhasin, B. A. Malomed, and R. Driben, J. Phys. B **38**, 877 (2005).

[31] J. Kasprzak, M. Richard, S. Kundermann, A. Baas, P. Jeambrun, J. M. J. Keeling, F. M. Marchetti, M. H. Szymańska, R. André, J. L. Staehli, V. Savona, P. B. Littlewood, B. Deveaud, and L. S. Dang, Nature **443**, 409 (2006).

[32] I. Carusotto and C. Ciuti, Rev. Mod. Phys. **85**, 299 (2013).

[33] O. L. Berman, Y. E. Lozovik, and D. W. Snoke, Phys. Rev. B **77**, 155317 (2008); O. L. Berman, G. Gumbs, and R. Ya. Kezerashvili, *ibid.* **96**, 014505 (2017).

[34] H. Min, R. Bistritzer, J.-J. Su, and A. H. MacDonald, Phys. Rev. B **78**, 121401 (2008).

[35] M. Sich, D. N. Krizhanovskii, M. S. Skolnick, A. V. Gorbach, R. Hartley, D. V. Skryabin, E. A. Cerda-Méndez, K. Biermann, R. Hey, and P. V. Santos, Nat. Photonics **6**, 50 (2012); D. Tanese, H. Flayac, D. Solnyshkov, A. Amo, A. Lemaître, E. Galopin, R. Braive, P. Senellart, I. Sagnes, G. Malpuech, and J. Bloch, Nat. Commun. **4**, 1749 (2013); E. A. Cerda-Méndez, D. Sarkar, D. N. Krizhanovskii, S. S. Gavrilov, K. Biermann, M. S. Skolnick, and P. V. Santos, Phys. Rev. Lett. **111**, 146401 (2013).

[36] Y. V. Kartashov and D. V. Skryabin, Optica **3**, 1228 (2016); Z. Wang, B. Wang, H. Long, K. Wang, and P. X. Lu, J. Lightwave Tech. **35**, 2960 (2017).